Data assimilation methods for urban air quality at the local scale

Chi Vuong Nguyen, Lionel Soulhac

Data assimilation methods for urban air quality at the local scale

Chi Vuong Nguyen[a,*], Lionel Soulhac[a]

[a]Laboratoire de Mécanique des Fluides et d'Acoustique, University of Lyon, CNRS UMR 5509 Ecole Centrale de Lyon, INSA Lyon, Université Claude Bernard, 36, avenue Guy de Collongue, 69134 Ecully, France

ARTICLE INFO

Keywords:
Air quality
Data assimilation
Urban dispersion model

ABSTRACT

Despite their wide applications in many fields of environmental sciences, data assimilation methods are still poorly adopted for the numerical simulation of pollutant dispersion at the local urban scale. In this study, we compare three data assimilation methods to evaluate the air quality at the local urban scale. The data assimilation methods used here are the Bias Ajustment Techniques, the Best Linear Unbiased Estimator, and the Source Apportionment Least Square method. We assess their performances on air pollution simulations in Lyon for the year 2008, focusing on ground-level NO_2 hourly concentrations. The results indicate that the three methods improve air quality estimates and that their performances are similar. This study shows that data assimilation is a promising tool to ameliorate air quality simulations at the urban scale.

1. Introduction

The estimate of air pollutant concentrations in urban areas is essential for different purposes, such as checking compliance with regulatory threshold levels (UNION et al., 2008), implementing actions and informing population when these levels are exceeded (Rouil et al., 2009), locating concentration thresholds exceedances, or even assessing pollutant human exposure in epidemiologic studies (Jacquemin et al., 2013; Morelli et al., 2016; Coudon et al., 2018; Coudon, 2018; Coudon et al., 2019; Danjou et al., 2019). Pollutant concentration used as reference air quality levels are usually those collected at monitoring stations. These however provide concentrations in a limited number of locations. To obtain a broader view on air quality it is therefore necessary to exploit numerical models, whose results enable to assess impact of emissions scenarii (Saikawa et al., 2011), reconstruct air pollution level in the past (Coudon et al., 2018, 2021), and forecast air pollution (Munoz-Alpizar et al., 2017; Zhou et al., 2017).

As is customary in several fields, the performances of these numerical models can be in principle improved using the information provided by field measurements adopting data assimilation (DA) methods. These latter are nowadays widely used in earth sciences (Ghil and Malanotte-Rizzoli, 1991; Kalnay, 2003; Navon, 2009), signal treatment (Goosse et al., 2012), or even in economics (Nadler et al., 2019). One of the most known application is certainly that in the field of atmospheric physics, notably in meteorology (Morel and Talagrand, 1974; McPherson, 1975; Miyakoda et al., 1976; McPherson et al., 1979). Applications of DA methods to air quality problems arose only in the late 1990s (Elbern et al., 1997; Elbern and Schmidt, 1999; Elbern et al., 2000; Segers et al., 2000; van Loon et al., 2000), and are today common for simulations at the mesoscale (Denby et al., 2008; Wu et al., 2008; Frydendall et al., 2009; Candiani et al., 2009). Conversely, they have been rarely used with urban dispersion models. As far as we are aware, only Tilloy et al. (2013) and Denby and Pochmann (2007) attempted to couple these methods with an urban air quality model.

To further investigate the ability of such methods to improve urban air quality estimates, we compare here the performances of three data assimilation methods, namely the Bias Ajustment Techniques (BAT), the Best Linear Unbiased Estimator (BLUE), and the Source Apportionment Least Square (SALS) method. The case study is the air quality within the Lyon agglomeration for the year 2008, using the hourly NO_2 concentration as target variable. Numerical simulation of the NO_2 concentrations were obtained with SIRANE (Soulhac et al., 2011), an atmospheric dispersion model for urban air quality.

In what follows, we begin by presenting the three data assimilation methods (section 2). The SIRANE urban air quality model is then introduced in the section 3 and the case study is presented in the section 4. The performances of the data assimilation methods are assessed in the section 5. The main findings of the study are summarized in the section 6.

2. Data assimilation methods

The objective of the DA methods is to estimate the state of a system (by definition unknown), represented by a state vector $\mathbf{x^t}$ ('t' stand for *true*) and generally referred to as *true state*. To estimate $\mathbf{x^t}$, DA methods rely on data provided by models and measurements. The former constitutes the *a priori* estimate of the system state. These data are represented by a state vector $\mathbf{x^b}$ ('b' stand for *background*) referred to as *background*. The two state vectors, $\mathbf{x^t}$ and $\mathbf{x^b}$, have size n. The measurements are usually represented by a vector $\mathbf{y}$ referred to as *observation vector*, of size m. Generally, m is significatively smaller than n (Daget, 2007).

Note that the values included in $\mathbf{y}$ may refer to a physical variable representing a proxy of the variable that constitutes the object of the study ($\mathbf{x^t}$ and $\mathbf{x^b}$). The observations can for example be the radiances measured by a satellite, whereas the background is relative to temperatures. Similarly, when

*Corresponding author
chi-vuong.nguyen@ec-lyon.fr (C.V. Nguyen);
lionel.soulhac@ec-lyon.fr (L. Soulhac)
ORCID(s): 0000-0003-0358-3486 (L. Soulhac)

including information on a same physical variable, data may refer to different spatial or temporal resolutions. Observations can for example concern time-varying concentrations, whereas the background is associated to concentration averaged on time. To compare the observation vector and the state vectors, it is necessary to define the so called *observation operator* to pass from the system space (space relative to state vectors) to the observations space. This operator is represented by the matrix $\mathbf{H}$ of size $m \times n$ (in what follows, we assume $\mathbf{H}$ to be linear). So, the equivalent of the true state and the background in the observation space are $\mathbf{Hx^t}$ and $\mathbf{Hx^b}$ respectively.

By combining the observations and the background, DA methods lead to the best estimate of the system state, represented by a state vector $\mathbf{x^a}$, referred to as *analysis* (also of size n). Likewise, the equivalent of the analysis in the observation space is $\mathbf{Hx^a}$.

In what follows we provide the details of the three methods used in this study: BAT, BLUE, and SALS.

2.1. Bias Adjustment Techniques (BAT)

The Bias Adjustment Techniques are relatively simple and aim at removing the bias of the background with respect to the true state, in order to have an unbiased analysis, i.e.:

$$\overline{\mathbf{x^t} - \mathbf{x^a}} = 0 \tag{1}$$

Observations are supposed to be unbiased with respect to the true state ($\overline{\mathbf{y} - \mathbf{Hx^t}} = 0$), so that BAT methods seek to estimate an analysis $\mathbf{x^a}$ verifying:

$$\overline{\mathbf{y} - \mathbf{Hx^a}} = 0 \tag{2}$$

BAT can be classified into two approaches: i) additive (McKeen et al., 2005; Wilczak et al., 2006; Kang et al., 2008; Monteiro et al., 2013) and ii) multiplicative (McKeen et al., 2005; Borrego et al., 2011; Monteiro et al., 2013). In this study, only the multiplicative approach is used, since it has the advantage of guaranteeing the positiveness of the estimates. With the multiplicative BAT, at each time step, the analysis is determined as:

$$\mathbf{x^a} = \mathbf{x^b} \frac{\overline{\mathbf{y}}}{\overline{\mathbf{Hx^b}}} \tag{3}$$

where $\overline{\mathbf{x}}$ represents a spatial average of the vector $\mathbf{x}$.

2.2. Best Linear Unbiased Estimator (BLUE)

The Best Linear Unbiased Estimator method (Blond et al., 2003; Tilloy et al., 2013) is a statistical interpolation method which determines the analysis with respect to the background and observation errors. The observation errors include errors due to the measurement instrument and those in the modelling of $\mathbf{H}$. With this method, the analysis $\mathbf{x^a}$ is expressed as:

$$\mathbf{x^a} = \mathbf{x^b} + \mathbf{K}\left(\mathbf{y} - \mathbf{Hx^b}\right) \tag{4}$$

where $\mathbf{K}$ is the *Kalman gain* matrix, defined as:

$$\mathbf{K} = \mathbf{BH}^{\mathrm{T}}(\mathbf{HBH}^{\mathrm{T}} + \mathbf{R})^{-1} \tag{5}$$

with $\mathbf{B}$ and $\mathbf{R}$ the *background errors covariance matrix* and *observation errors covariance matrix*, respectively.

The modelling of theses matrices, especially the matrix $\mathbf{B}$, constitutes the critical step of the BLUE method. In this study, these matrices are stationary (time-independent). Note that this method does not guarantee the positiveness of the estimates. Therefore eventual negative values are replaced by zeros.

2.2.1. *Matrix* R

The matrix $\mathbf{R}$ represents the *observation errors covariance matrix*. In this study, the observation errors between two different points p_i and $p_{j\neq i}$ are considered as uncorrelated (Blond et al., 2003; Tombette et al., 2009; Wang et al., 2011; Silver et al., 2013; Tilloy et al., 2013), as is the case of observations at different points with different instruments (Tilloy et al., 2013). With this assumption, the matrix $\mathbf{R}$ is diagonal. Moreover we assume that the observation errors are normally distributed and that 95 % of these errors are smaller than a given percentage (equivalent to the uncertainty of the measurement) of the average concentration. The matrix $\mathbf{R}$ is then modelled as:

$$\begin{aligned} &\mathbf{R} = \mathrm{diag}(\sigma_1^2, \sigma_2^2, ..., \sigma_m^2) \\ &\text{with } 1.96\sigma_i = \frac{\delta_i}{T} \sum_t^T y_{i,t} \end{aligned} \tag{6}$$

where $y_{i,t}$ represents the measured concentration at the i^{th} monitoring station at time t, δ_i is the related uncertainty and T is the number of time steps. In this case study, the uncertainty is fixed equal to 15 %, as suggested by the 2008 regulatory directive on air quality (UNION et al., 2008).

2.2.2. *Matrix* B

The matrix $\mathbf{B}$ represents the *background errors covariance matrix*. We assume here that the background errors associated to points p_i and p_j are more correlated when these points are impacted by the same events (Blond et al., 2003), i.e. when the background associated to p_i and p_j are more correlated. So, the background errors covariance B_{ij} is modelled as a function of the background correlation coefficient ρ_{ij}^{b} and the (background) variances $\sigma_i^{2,\mathrm{b}}$ and $\sigma_j^{2,\mathrm{b}}$ as:

$$\begin{aligned} &\mathrm{B}_{ij} = \sqrt{\sigma_i^{2,\mathrm{z}} \sigma_j^{2,\mathrm{z}}}\, \rho_{ij}^{\mathrm{z}} \\ &\text{with} \begin{cases} \sigma_i^{2,\mathrm{z}} = \alpha \sigma_i^{2,\mathrm{b}} \\ \rho_{ij}^{\mathrm{z}} = \rho_0 \exp\left(\dfrac{\rho_{ij}^{\mathrm{b}} - 1}{L_\rho}\right) \end{cases} \end{aligned} \tag{7}$$

where the parameters α, ρ_0 and L_ρ represent an adjustment coefficient, a characteristic correlation coefficient, and a characteristic correlation length, respectively. These parameters

are determined by seeking those that satisfy the χ^2 diagnostic (Ménard and Chang, 2000; Tombette et al., 2009; Tilloy et al., 2013). Among these, we chose here the combination leading to the lower quadratic error, following a cross-validation.

2.3. Source Apportionment Least Square (SALS)

Source apportionment methods aim at estimating the contribution to air pollution by different 'groups' of sources. Typically, the groups of sources can be defined according to their typology (e.g. traffic, industry, agriculture or residential-tertiary emissions), their location (e.g. emissions from different regions of Europe), and/or their emissions period (emissions in different seasons).

The Source Apportionment Least Square (SALS) method (Nguyen et al., 2018) assumes that uncertainties associated to predictions by air quality models are mainly due to emission estimates. Therefore, the SALS method essentially correct (indirectly) emission data in order to improve air quality models estimates. This correction is achieved by modulating, in an optimal way, the sources contributions. The background is then expressed as:

$$\mathbf{x^b} = \sum_{g}^{G} \mathbf{x}_g^{\mathbf{b}} \tag{8}$$

where G is the number of sources groups and $\mathbf{x}_g^{\mathbf{b}}$ represent the background associated to the contribution of the group g. Likewise, the SALS method determines (at each time step) the analysis $\mathbf{x^a}$ as a linear combination of sources contributions:

$$\mathbf{x^a} = \sum_{g}^{G} \alpha_g \mathbf{x}_g^{\mathbf{b}} \tag{9}$$

where α_g represent the modulation coefficient associated to the group g. The best estimate minimizes the quadratic error with respect to observations, which are supposed to be 'perfect' ($\mathbf{y} = \mathbf{H}\mathbf{x^t}$), i.e. not affected by uncertainties. The coefficients α_g are evaluated (at each time step) by minimizing the cost function:

$$J(\alpha_1, \alpha_2, ..., \alpha_G) = \left(\mathbf{y} - \sum_{g}^{G} \alpha_g \mathbf{H}\mathbf{x}_g^{\mathbf{b}}\right)^{\mathrm{T}} \left(\mathbf{y} - \sum_{g}^{G} \alpha_g \mathbf{H}\mathbf{x}_g^{\mathbf{b}}\right) \tag{10}$$

where m is the number of available measurements at the analysis time. The coefficients α_g are determined by solving the system:

$$\begin{pmatrix} (\mathbf{H}\mathbf{x}_1^{\mathbf{b}})^{\mathrm{T}}(\mathbf{H}\mathbf{x}_1^{\mathbf{b}}) & \dots & (\mathbf{H}\mathbf{x}_1^{\mathbf{b}})^{\mathrm{T}}(\mathbf{H}\mathbf{x}_G^{\mathbf{b}}) \\ \vdots & \ddots & \vdots \\ (\mathbf{H}\mathbf{x}_G^{\mathbf{b}})^{\mathrm{T}}(\mathbf{H}\mathbf{x}_1^{\mathbf{b}}) & \dots & (\mathbf{H}\mathbf{x}_G^{\mathbf{b}})^{\mathrm{T}}(\mathbf{H}\mathbf{x}_G^{\mathbf{b}}) \end{pmatrix} \begin{pmatrix} \alpha_1 \\ \vdots \\ \alpha_G \end{pmatrix} = \begin{pmatrix} \mathbf{y}^{\mathrm{T}}(\mathbf{H}\mathbf{x}_1^{\mathbf{b}}) \\ \vdots \\ \mathbf{y}^{\mathrm{T}}(\mathbf{H}\mathbf{x}_G^{\mathbf{b}}) \end{pmatrix} \tag{11}$$

When the number of observations m is larger than the number of sources groups G, the estimate of the coefficients α_g is based on a least square problem. The SALS method is applied only when $m \geq G$. In this method we assume that the sources groups contributions are positive (or null). The solution of the system (11) is then obtained with the Lawson and Hanson (1974) method, which guarantees that the coefficients α_g are positive.

3. The SIRANE model

SIRANE is an operational model simulating pollutants dispersion at local urban scale, assuming steady meteorological conditions over hourly time steps (Soulhac et al., 2011). It is based on the street network concept (Soulhac et al., 2011; Soulhac, 2000) and adopts parametric laws to model the main flow and dispersion processes within an urban area (Soulhac et al., 2013): convective transport along the street (Soulhac et al., 2008), turbulent transfer at roof level (Salizzoni et al., 2009, 2007), and exchanges at the street intersections (Soulhac et al., 2009). The presence of a roughness sub-layer just above the urban canopy (above roof level) is neglected and the flow is modelled as a surface boundary layer over a rough surface. There, the pollutants dispersion is modelled by a Gaussian puff model, with ground reflection, whose standard deviations are parametrised according to the Monin-Obukhov similarity theory. The only chemical reactions taken into account in SIRANE concern the NO_2-NO-O_3 cycle, computed assuming a photo-stationary equilibrium (Seinfeld, 1986). The input data of the SIRANE model are the urban geometry, the meteorological data, the locations and the modulations of the emissions (represented as point, line, and surface sources) and the hourly evolution of the background concentrations, i.e. the concentrations due to pollutants coming from outside the domain. SIRANE has been validated against wind tunnel experiments (Salem et al., 2015; Carpentieri et al., 2012; Soulhac, 2000) and on-site measurements (Bo et al., 2020b,a; Pognant et al., 2018; Soulhac et al., 2017, 2012). Futher details on the SIRANE model can be found in Soulhac et al. (2017, 2011).

4. The case study

The performances of the three DA methods are evaluated on the case study previously used to assess the performances of the SIRANE 2.0 model (Soulhac et al., 2017). We consider NO_2 hourly mean concentrations (at ground-level) in the Lyon urban agglomeration, a 36 km × 40 km domain (represented with a spatial resolution of 10 m in the SIRANE simulation), for the year 2008. Time-series of NO_2 hourly mean concentrations used to assess the performances of the DA were collected in 16 monitoring stations (fig. 1) by Atmo Auvergne Rhône Alpes, the local authority for air quality. These stations can be classified in four distinct categories: background stations (Côtières de l'Ain, Genas, Saint-Exupéry, and Ternay), stations located on high-intensity traf-

Table 1
Statistical indices and quality criteria used to assess estimates (c_m is the measured concentration and c_p is the predicted concentration)

	Bias	RMSE	r
Definition	$\overline{c_m - c_p}$	$\sqrt{\overline{(c_m - c_p)^2}}$	$\frac{\overline{(c_m - \overline{c_m})(c_p - \overline{c_p})}}{\sqrt{\overline{(c_m - \overline{c_m})^2}\,\overline{(c_p - \overline{c_p})^2}}}$
Criteria	$\lvert\text{Bias}\rvert \leq 0.33\,\overline{c_m}$	$\text{RMSE} \leq \overline{c_m}$	$r \geq 0.60$

fic roads (Berthelot, Garibaldi, Grand-Clément, Lyon Périphérique, Mulatière, and Vaise), stations placed close to industrial sites (Feyzin and Saint-Fons) and stations within the urban agglomeration and away from high-intensity traffic roads (Gerland, Lyon Centre, Saint-Just, and Vaulx-en-Velin). In this dataset, missing hourly data do not exceed 3 % over the whole year 2008. For this study, the DA methods combine these measurements with the SIRANE estimates.

To evaluate the reliability of the models results, three statistical indices are used: the bias, Root Mean Square Error (RMSE), and correlation coeffficient (r). The definition of these statistical indices is given in table 1, where are also reported the criteria according to which we can consider as

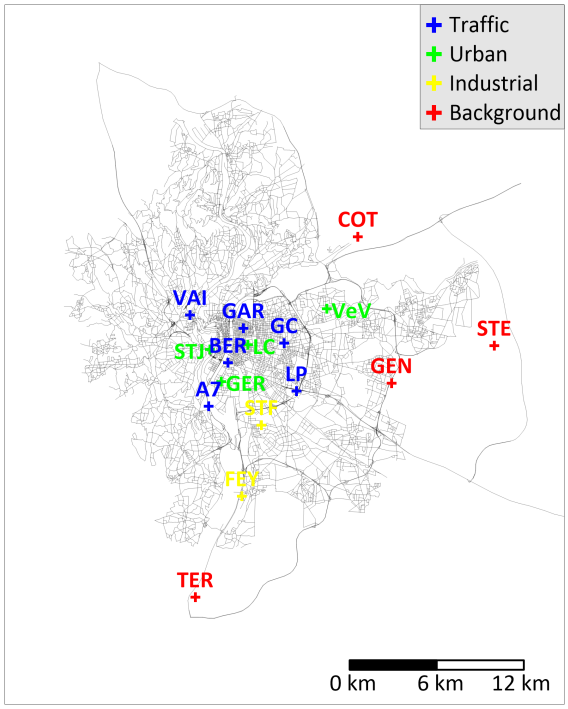

Figure 1: Study domain and localisation of the monitoring stations (A7: Mulatière, BER: Berthelot, COT: Côtière de l'Ain, FEY: Feyzin, GAR: Garibaldi, GC: Grand-Clément, GEN: Genas, GER: Gerland, LC: Lyon Centre, LP: Lyon Périphérique, STE: Saint-Exupéry, STF: Saint-Fons, STJ: Saint-Just, TER: Ternay, VAI: Vaise, VeV: Vaulx-en-Velin)

'good' the model performances. Note that these criteria are more restrictive than those proposed by Chang et al. (2005) and Chang and Hanna (2004) (Nguyen, 2017) that are usually adopted in the literature.

5. Result

5.1. Background evaluation

The quality of the background (SIRANE results) are reported on figure 2, which respresents the bias, RMSE, and correlation coefficients compared to the measured average concentrations. The bias is generally positive. This means that SIRANE globally underestimates the concentrations. Nevertheless, the bias criteria is validated for all stations. The RMSE exhibits a nearly linear relation with the measured average concentrations. The larger is the measured average concentration, the higher is the RMSE. Note however that the RMSE criteria is validated for all stations. Inversely, the lower is the measured average concentration the higher is the correlation coefficient. The only station which does not meet the correlation coefficient criteria is an industrial station (Feyzin). Globally, the background fullfills the quality criteria for these statistical indices. However, background errors are sometimes significant, especially for the traffic stations.

The figure 2 shows that the performances for traffic stations are worse than those associated to background, industrial, and urban stations. Results highlight the general tendency of SIRANE in strong underestimating pollutant concentrations (positive bias) at traffic stations. These underestimations are independent of the location of the receptors and concern evenly monitoring stations placed in 'open field' (Garibaldi, Grand-Clément, Lyon Périphérique et Mulatière) and within street canyons (Berthelot et Vaise). Therefore, the discrepancies between modelled and measured concentrations cannot be specifically associated to the parametric laws used to model pollutant transfer within the urban canopy. A potential explanation for these discrepancies is related to vehicles emissions factors. Previous authors (Smit et al., 2008; Berkowicz et al., 2006) suggest that these factors are underestimated. Lately, O'Driscoll et al. (2016) indicate that COPERT modelling results for Euro 6 diesel cars noticeably under predict NO_2 and NOx emissions. Likewise, Jaikumar et al. (2017) show that the real emissions are underestimated

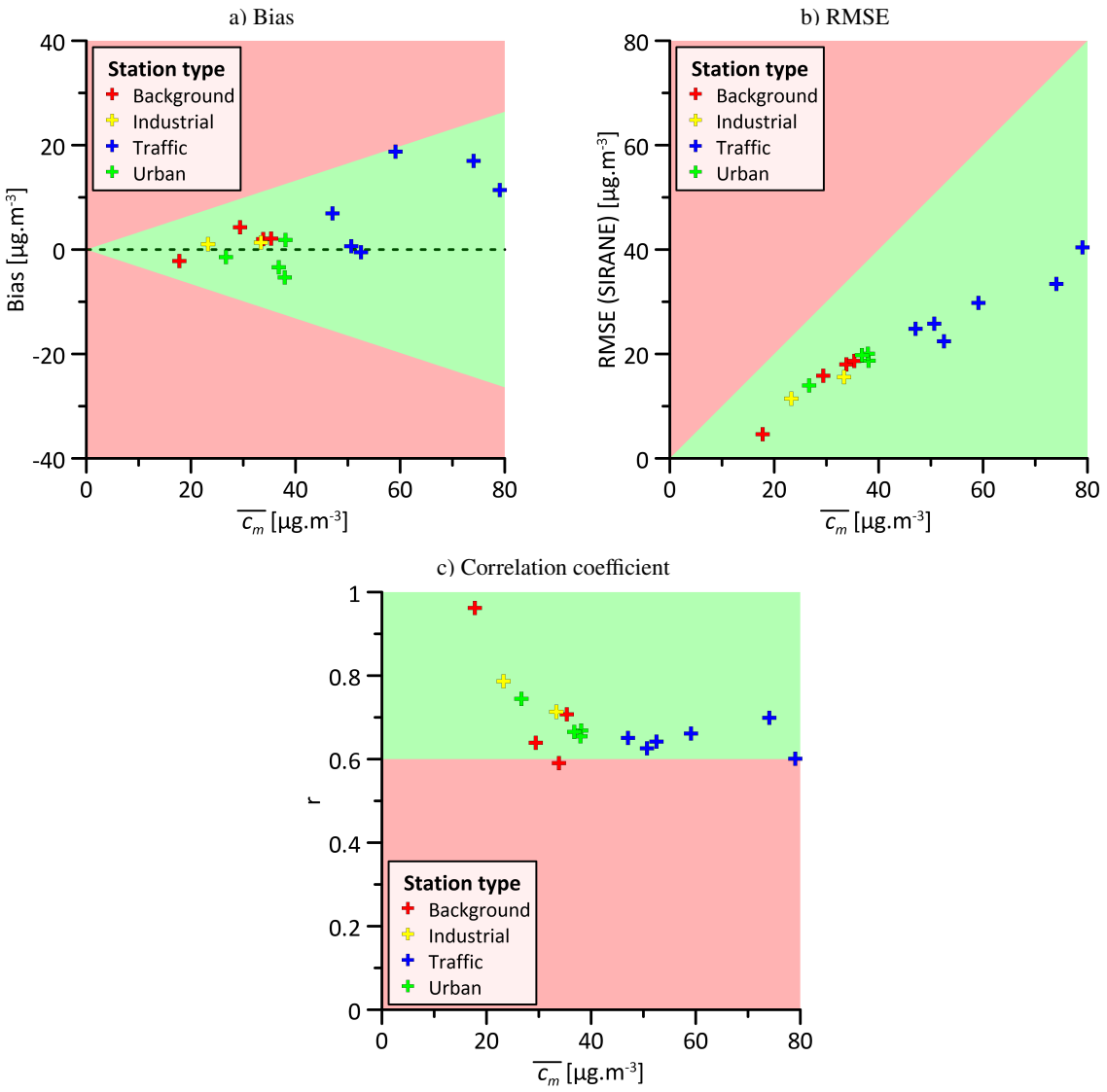

Figure 2: Bias (a), RMSE (b) and correlation coefficient (c) compared to the measured average concentrations for the background (SIRANE results). Green (red) areas indicate that the results respect (do not respect) the quality criteria.

by 30-200 %, depending upon different driving modes, with the standard emission models (like COPERT).

Soulhac et al. (2017) provide possible explanations about the lower performances related to Vaise and Mulatière stations. The location of the Vaise station can explain its low results. This station is located in a district actually bordered by two hills. This forms a small valley where the air circulation is somehow decoupled to that occurring in the rest of the city. This morphological configuration can lead to an accumulation of pollutant within the district, due to the recirculation flows occurring in this small valley. This complex air circulation is not simulated by the SIRANE meteorological preprocessing, which assumes that the flow over the whole urban area is homogeneous on the horizontal plane. Therefore, SIRANE is not able to model these effects inducing an accumulation of air pollutant within this district. Its predictions tend then to systematically underestimate real concentration values. Concerning Mulatière station, Soulhac et al. (2017) highlight the influence of the stability condition. They indicate that for unstable conditions the model performances are significantly deteriorated. The figure 6 shows in particular the correspondence of negative peaks of L_{MO}^{-1} (inverse of the Monin-Obukhov length), i.e strong unstable conditions, with a systematic underestimation of the measured concentration, and that the model is unable to reproduce the peak characterising the morning rush hour. This is likely due to the parameterisation of the plume width in case of strongly unstable atmospheric conditions which over predicts the dispersion and the mixing close to the source.

5.2. DA performances

The performances of the DA methods are assessed by means of a leave-one-out cross-validation, i.e. by estimating the concentrations at one station using all measurements, except those of this same station. This procedure is repeated for all stations and the estimates are compared to the mea-

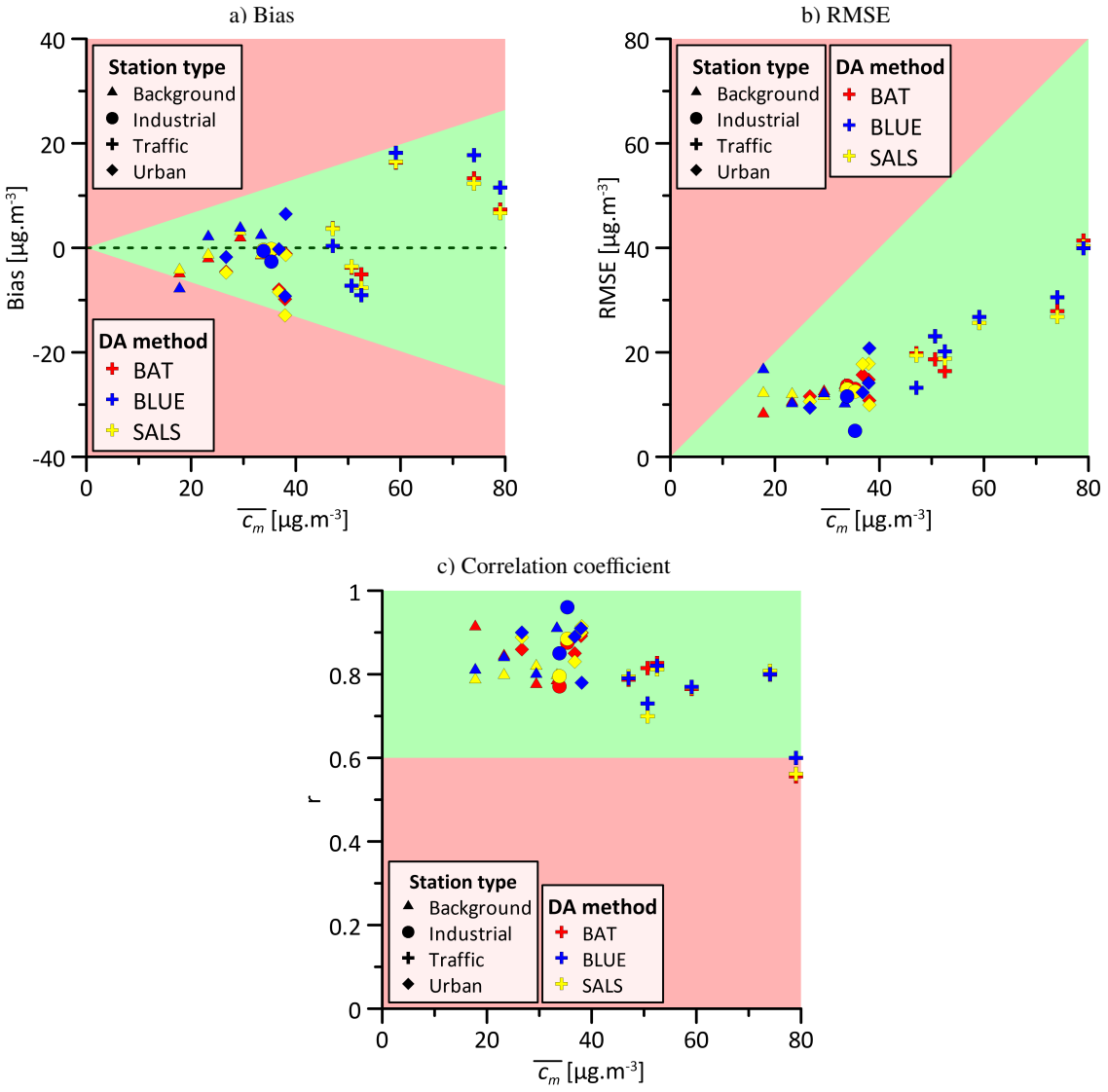

Figure 3: Bias (a), RMSE (b) and correlation coefficient (c) compared to the measured average concentrations for the analysis from the DA methods. Green (red) areas indicate that the results respect (do not respect) the quality criteria.

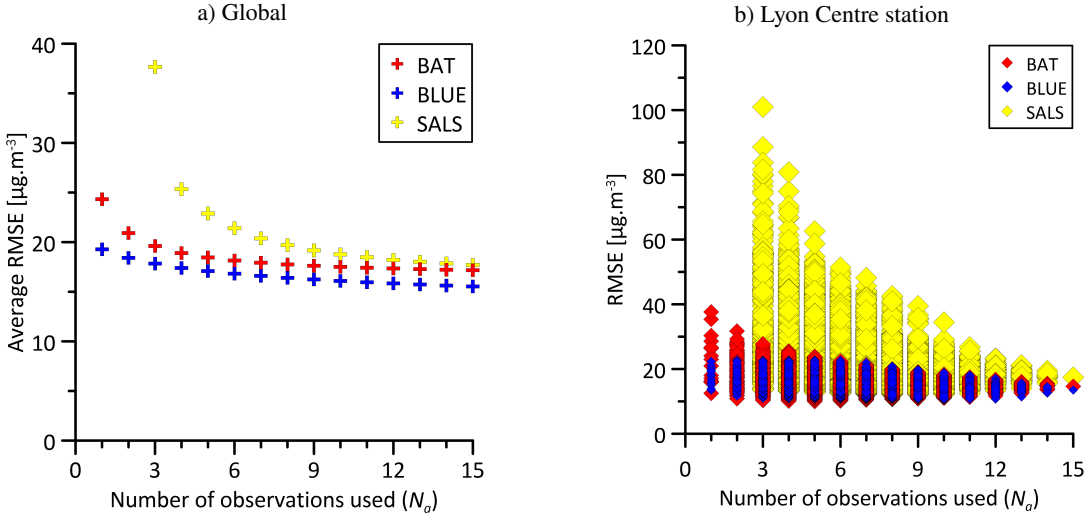

Figure 4: Variation of the average RMSE for all stations (a) and for Lyon Centre station (b) compared to the number of observations used (N_a)

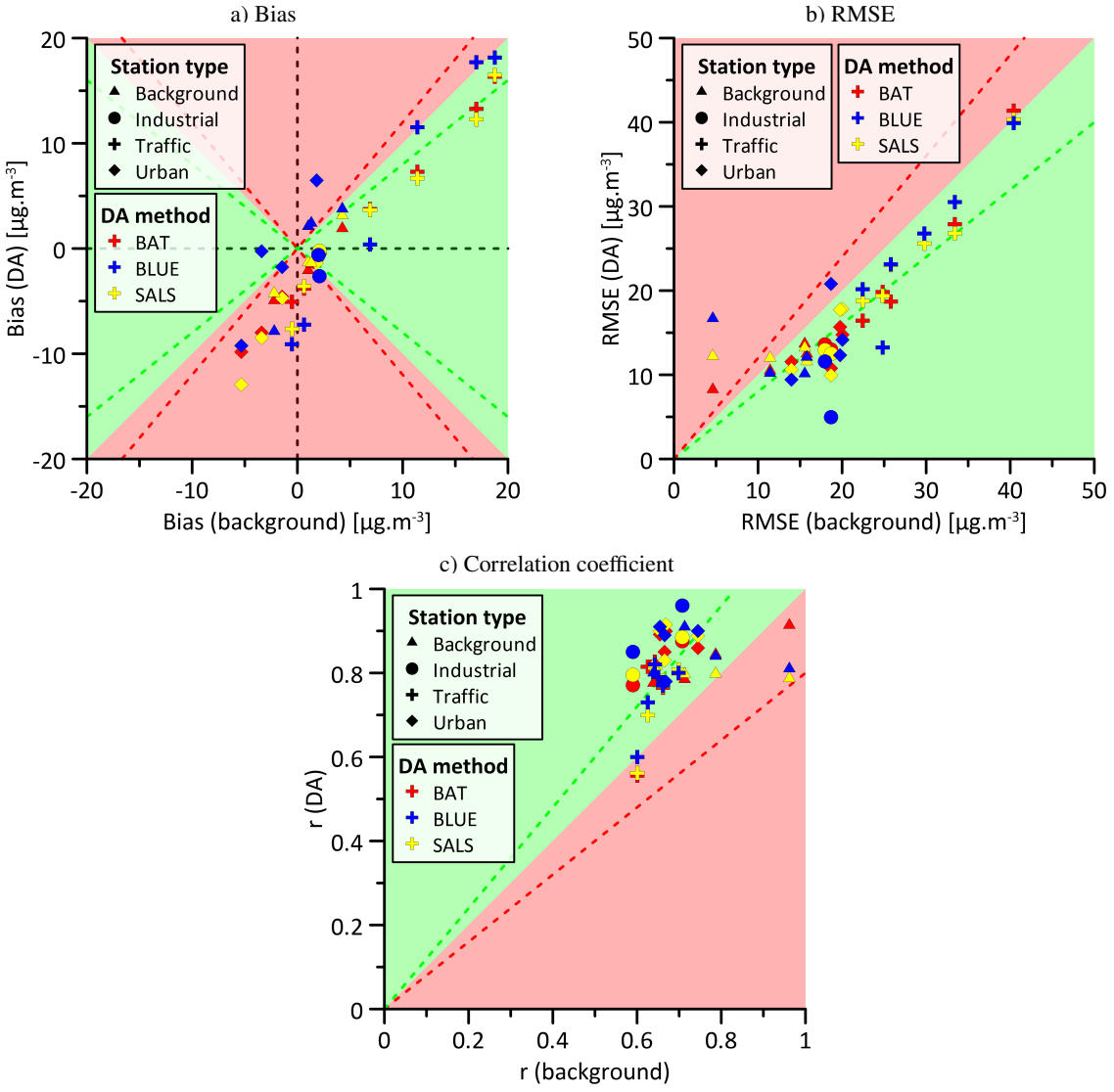

Figure 5: Bias (a), RMSE (b) and correlation coefficient (c) before (background) and after DA. Green (red) areas indicate that the results are better (worse) after DA. The dashed lines delineate 20 % improvement - decline of the statistical indices.

surements. This approach aims at evaluating the quality of the estimates from the DA methods where no observations are available. Here, the SALS method is implemented considering three groups of sources: i) the traffic contribution, ii) the heat emissions, and iii) the industrial emissions with the background concentration. These contributions are evaluated with the SA-NOX SIRANE module (Nguyen et al., 2018). The parameters used to model the matrix $\mathbf{B}$ are $\rho_0 = 0.75$, $L_\rho = 0.05$, and $\alpha = 0.95$.

The figure 3 shows the bias, RMSE, and correlation coefficients compared to the measured average concentrations for the analysis from the three DA methods. Unlike background (SIRANE), there is an almost balanced ditribution of negative and positive bias with the three DA methods. The bias criteria is validated for all stations, except for one station with the BLUE and SALS method. As for background, the RMSE exhibits a nearly linear relation between the RMSE and the measured average concentrations. With the three DA methods, the RMSE criteria is validated for all stations. Likewise, the correlation coefficients validate the quality criteria for all stations, except one (Mulatière traffic station). Statistically, the performances of the three DA methods are globally *good* and similar to each other. Nevertheless, the errors after the application of DA can still be significant. Note that like background, figure 3 highlights that the results for traffic stations are worse than those related to background, industrial and urban stations.

To assess the influence of the number of measurements used during the assimilation (N_a), the concentrations are evaluated (with the DA methods) for each station, using measurements provided by N_a others stations (with a cross-validation approach), which are identical for each time step ($N_a = 1, 2, ..., m-1$). This is done for all possible combinations of N_a stations. Note that this assessment is done only for the time steps at which measurements are available at all (m) stations. The figure 4.a shows the average RMSE compared

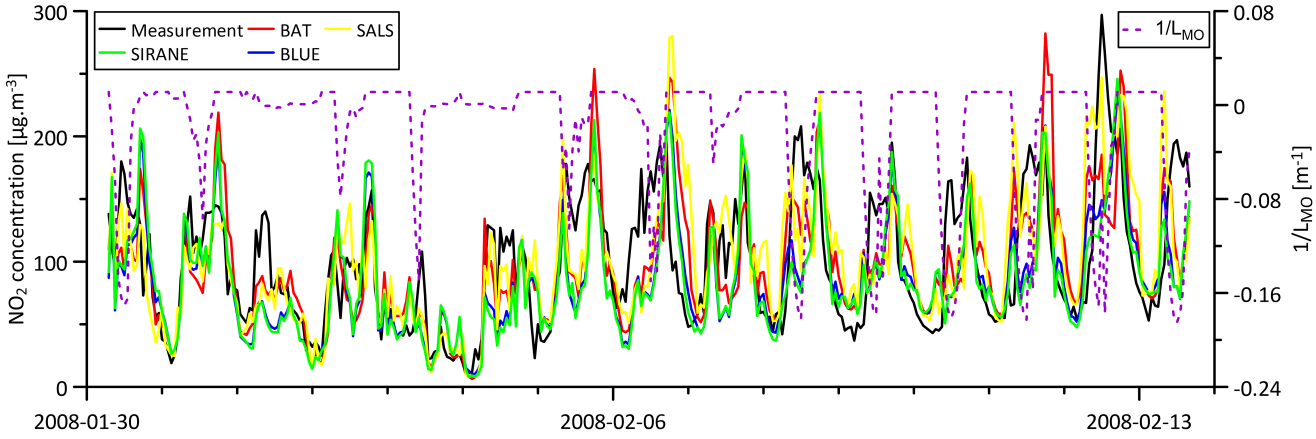

Figure 6: Measured and modelled concentrations at Mulatière station superposed with the evolution of the inverse of the Monin-Obukhov length

to N_a for the three DA methods (here *average RMSE* means that, for each N_a value, all the RMSE obtained by assimilating N_a measurements are averaged regardless the station). Globally, the higher is the number of observations used, the smaller is the average RMSE for the three DA methods. This confirms the results by Denby and Pochmann (2007), who enlighted that DA is more efficient as the number of observations increases. The average RMSE decreases by 20.0 $\mu g.m^{-3}$ between $N_a = 3$ and $N_a = 15$ with the SALS method. With the BAT and BLUE methods, the RMSE decreases by 7.1 $\mu g.m^{-3}$ and 3.7 $\mu g.m^{-3}$ respectively between $N_a = 1$ and $N_a = 15$. However, from a given N_a value (approximately from $N_a = 9$), the RMSE does not further decrease and attains a constant value for both the BAT (RMSE = 17.2 $\mu g.m^{-3}$) and BLUE (RMSE = 15.5 $\mu g.m^{-3}$) methods. Denby and Pochmann (2007) used a kriging approach (Cressie, 1993) and pointed out that the DA provides more reliable concentration estimates when their spatial variability occurs over a spatial scale exceeding the distances between the measurements stations. In our case, this does not hold because concentration variations occur on typical spatial scale of tens of meters, whereas the distance between the two closest stations is about 1.2 km (the average distance between the stations is about 9.7 km). This can explain why the average RMSE does not further decrease from $N_a = 9$, especially with the BLUE method. The figure 4.a also indicates that the average RMSE are better with the BLUE method. Moreover, the variation of the average RMSE is less sensitive to N_a with the BLUE method than with the SALS and BAT methods. The figure 4.b shows the RMSE compared to N_a, obtained with all the combinations, for Lyon Centre station. Results indicate that the RMSE associated to $N_a = m - 1$ is higher than the RMSE obtained with some combinations involving lower N_a measurements. The best RMSE is associated to a combination of $N_a = 9$ and $N_a = 5$ measurements for the BLUE and BAT methods, respectively. Likewise, for each N_a value, the RMSE varies sometimes significantly compared to the combinations of stations used. We can then conclude that the number of observations and the characteristics of the measurements both influence the efficiency of the DA. These results suggest that there are combinations of stations that are more reliable than other.

5.3. DA versus background

In figure 5 we compare the bias, RMSE, and correlation coefficients computed before (background) and after the application of DA. DA methods mainly improves the bias which are initially higher and positive, especially those associated to traffic stations. In the other hand, bias are generally worse after DA for background, industrial and urban stations. We note that only the BLUE method improves the bias which are initially negative and positive (BAT and SALS methods improve only bias which are initially positive). This shows that this method is able to *correct* the background in cases with spatially non-uniform bias. Once applied DA, the RMSE and the correlation coefficients improve of approximately 20 %, regardless of the DA method. Note however that the improvement of these two statistical indices is globally slightly lower for traffic stations. Measured concentrations at these stations are strongly influenced by local nearby effects (e.g. traffic emssions). Therefore, it is more difficult to correct discrepancies for these stations using only measured concentrations from remote stations (DA is here carried out with a leave-one-out cross-validation approach). This is in line with the comments of Denby and Pochmann (2007) who indicate that the reliability of the DA depends on the spatial variability of the concentrations and the distance between the stations. Globally, the DA methods improve statistically the estimated concentrations. Note nevertheless that the improvements and the degradations are not uniform in space.

Soulhac et al. (2017) highlight the relation between the stability condition and the discrepancies between measured and modelled concentrations, especially for Mulatière traffic station. The figure 6 presents two weeks time series of measured and modelled NO_2 concentrations at Mulatière station where the evolution of L_{MO}^{-1} is also superposed. The results show that the DA methods sometimes manage to improve

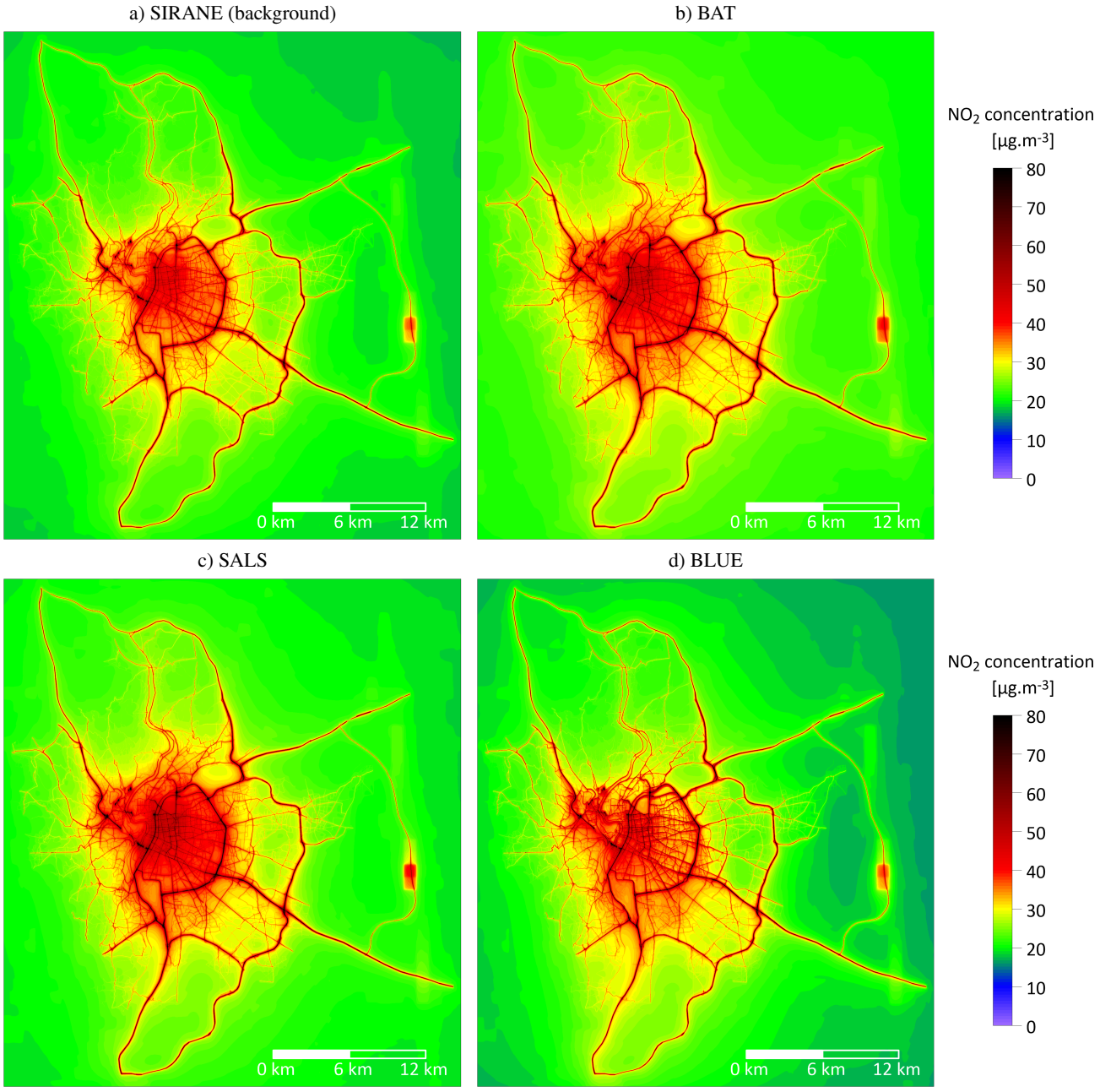

Figure 7: NO_2 mean concentration field within the Lyon urban agglomeration for the year 2008 estimated with SIRANE (a) and the three DA methods (b, c, and d)

the estimates when negative peaks of L_{MO}^{-1} (unstable conditions) occur, at which time the background (SIRANE) tends to underestimate the measured concentrations.

The figure 7 shows ground-level NO_2 concentration field (averaged over 2008) over the Lyon urban agglomeration, before and after DA (estimated without cross-validation). The concentration field obtained with the BAT and SALS methods are comparable. With these two DA methods the concentrations are slightly higher than with the background (SIRANE). Within the city centre, the concentrations are slightly lower with the BLUE method than with the two others DA methods. Although the three DA methods lead to similar statistical indices (after cross-validation), the NO_2 mean concentration field resulting from these DA methods are nevertheless slightly different.

6. Conclusion

In this study, we have assessed the performances of three data assimilation methods, namely BAT, BLUE, and SALS, in the evaluation of urban air quality. These methods have been applied with the SIRANE air quality model focusing on

NO_2 hourly mean concentrations in the Lyon agglomeration for the year 2008.

The statistical performances associated to DA methods are globally satisfactory and show that these methods can improve results of urban air quality models. Nonetheless, once applied DA, the errors can be worse than those obtained without applying it. Also, the improvement of the results is not spatially uniform and the best results is not always obtained with the same DA method.

Globally, the performances are similar for the three DA methods. Nevertheless, only the BLUE method improves bias that are spatially non-uniform. Generally, the predictions provided by these DA methods are improved increasing the number of observations. Compared to other methods, the BLUE method is however less sensitive to the number of measurements used. The estimates can sometimes be better using only few particular observations, suggesting that there are more relevant combinations of stations to use for DA. This feature can be the object of an optimisation network problem.

Acknowledgments

The authors would like to thank P. Salizzoni for carefully reading the paper and providing a critical review of its content.

References

Berkowicz, R., Winther, M., Ketzel, M., 2006. Traffic pollution modelling and emission data. Environmental Modelling & Software 21, 454–460.

Blond, N., Bel, L., Vautard, R., 2003. Three-dimensional ozone data analysis with an air quality model over the Paris area. Journal of Geophysical Research: Atmospheres 108.

Bo, M., Charvolin-Volta, P., Clerico, M., Nguyen, C.V., Pognant, F., Soulhac, L., Salizzoni, P., 2020a. Urban air quality and meteorology on opposite sides of the Alps: The Lyon and Torino case studies. Urban Climate 34, 100698.

Bo, M., Salizzoni, P., Pognant, F., Mezzalama, R., Clerico, M., 2020b. A Combined Citizen Science-Modelling Approach for NO2 Assessment in Torino Urban Agglomeration. Atmosphere 11, 721.

Borrego, C., Monteiro, A., Pay, M., Ribeiro, I., Miranda, A., Basart, S., Baldasano, J., 2011. How bias-correction can improve air quality forecasts over Portugal. Atmospheric Environment 45, 6629–6641.

Candiani, G., Carnevale, C., Pisoni, E., Volta, M., 2009. Assimilation of chemical ground measurements in air quality modeling, in: International Conference on Large-Scale Scientific Computing, Springer. pp. 157–164.

Carpentieri, M., Salizzoni, P., Robins, A., Soulhac, L., 2012. Evaluation of a neighbourhood scale, street network dispersion model through comparison with wind tunnel data. Environmental Modelling & Software 37, 110–124.

Chang, J.C., Hanna, S.R., 2004. Air quality model performance evaluation. Meteorology and Atmospheric Physics 87, 167–196.

Chang, J.C., Hanna, S.R., Boybeyi, Z., Franzese, P., 2005. Use of Salt Lake City URBAN 2000 field data to evaluate the urban hazard prediction assessment capability (HPAC) dispersion model. Journal of Applied Meteorology 44, 485–501.

Coudon, T., 2018. Développement et application de méthodologies d'évaluation des expositions atmosphériques chroniques aux dioxines et au cadmium dans le cadre d'études épidémiologiques. Ph.D. thesis. Lyon.

Coudon, T., Danjou, A.M.N., Faure, E., Praud, D., Severi, G., Mancini, F.R., Salizzoni, P., Fervers, B., 2019. Development and performance evaluation of a GIS-based metric to assess exposure to airborne pollutant emissions from industrial sources. Environmental Health 18, 8.

Coudon, T., Hourani, H., Nguyen, C., Faure, E., Mancini, F.R., Fervers, B., Salizzoni, P., 2018. Assessment of long-term exposure to airborne dioxin and cadmium concentrations in the Lyon metropolitan area (France). Environment international 111, 177–190.

Coudon, T., Nguyen, C.V., Volta, P., Grassot, L., Couvidat, F., Soulhac, L., Gulliver, J., Mancini, F.R., Fervers, B., Salizzoni, P., 2021. Retrospective modeling of no2 and pm10 concentrations over the lyon metropolitan area (france), 1990âĂŞ2010âĂŤperformance evaluation, exposure assessment and correlation between pollutants. Atmosphere 12. URL: https://www.mdpi.com/2073-4433/12/2/239, doi:10.3390/atmos12020239.

Cressie, N.A.C., 1993. Statistics for spatial data. J. Wiley.

Daget, N., 2007. Revue des méthodes d'assimilation .

Danjou, A.M.N., Coudon, T., Praud, D., Lévêque, E., Faure, E., Salizzoni, P., Le Romancer, M., Severi, G., Mancini, F.R., Leffondré, K., et al., 2019. Long-term airborne dioxin exposure and breast cancer risk in a case-control study nested within the French E3N prospective cohort. Environment international 124, 236–248.

Denby, B., Pochmann, M., 2007. Basic data assimilation methods for use in urban air quality assessment, in: Proceedings of the 6th International Conference on Urban Air Quality. Limassol, Cyprus, pp. 27–29.

Denby, B., Schaap, M., Segers, A., Builtjes, P., Horálek, J., 2008. Comparison of two data assimilation methods for assessing PM10 exceedances on the European scale. Atmospheric Environment 42, 7122–7134.

Elbern, H., Schmidt, H., 1999. A four-dimensional variational chemistry data assimilation scheme for Eulerian chemistry transport modeling. Journal of Geophysical Research: Atmospheres 104, 18583–18598.

Elbern, H., Schmidt, H., Ebel, A., 1997. Variational data assimilation for tropospheric chemistry modeling. Journal of Geophysical Research: Atmospheres 102, 15967–15985.

Elbern, H., Schmidt, H., Talagrand, O., Ebel, A., 2000. 4D-variational data assimilation with an adjoint air quality model for emission analysis. Environmental Modelling & Software 15, 539–548.

Frydendall, J., Brandt, J., Christensen, J.H., 2009. Implementation and testing of a simple data assimilation algorithm in the regional air pollution forecast model, DEOM. Atmospheric Chemistry & Physics Discussions 9.

Ghil, M., Malanotte-Rizzoli, P., 1991. Data assimilation in meteorology and oceanography, in: Advances in geophysics. Elsevier. volume 33, pp. 141–266.

Goosse, H., Guiot, J., Mann, M.E., Dubinkina, S., Sallaz-Damaz, Y., 2012. The medieval climate anomaly in Europe: Comparison of the summer and annual mean signals in two reconstructions and in simulations with data assimilation. Global and Planetary Change 84, 35–47.

Jacquemin, B., Lepeule, J., Boudier, A., Arnould, C., Benmerad, M., Chappaz, C., Ferran, J., Kauffmann, F., Morelli, X., Pin, I., et al., 2013. Impact of geocoding methods on associations between long-term exposure to urban air pollution and lung function. Environmental health perspectives 121, 1054.

Jaikumar, R., Nagendra, S.S., Sivanandan, R., 2017. Modal analysis of real-time, real world vehicular exhaust emissions under heterogeneous traffic conditions. Transportation Research Part D: Transport and Environment 54, 397–409.

Kalnay, E., 2003. Atmospheric modeling, data assimilation and predictability. Cambridge university press.

Kang, Y.S., Baik, J.J., Kim, J.J., 2008. Further studies of flow and reactive pollutant dispersion in a street canyon with bottom heating. Atmospheric environment 42, 4964–4975.

Lawson, C.L., Hanson, R.J., 1974. Linear least squares with linear inequality constraints. Solving least squares problems. Englewood Cliffs (NJ): Prentice-Hall. p 161.

van Loon, M., Builtjes, P.J., Segers, A., 2000. Data assimilation of ozone in the atmospheric transport chemistry model LOTOS. Environmental Modelling & Software 15, 603–609.

McKeen, S., Wilczak, J., Grell, G., Djalalova, I., Peckham, S., Hsie, E.Y., Gong, W., Bouchet, V., Menard, S., Moffet, R., et al., 2005. Assessment of an ensemble of seven real-time ozone forecasts over eastern North

America during the summer of 2004. Journal of Geophysical Research: Atmospheres 110.

McPherson, R., Bergman, K., Kistler, R., Rasch, G., Gordon, D., 1979. The nmc operational global data assimilation system. Monthly Weather Review 107, 1445–1461.

McPherson, R.D., 1975. Progress, problems, and prospects in meteorological data assimilation. Bulletin of the American Meteorological Society 56, 1154–1166.

Ménard, R., Chang, L.P., 2000. Assimilation of stratospheric chemical tracer observations using a Kalman filter. Part II: χ2-validated results and analysis of variance and correlation dynamics. Monthly weather review 128, 2672–2686.

Miyakoda, K., Umscheid, L., Lee, D., Sirutis, J., Lusen, R., Pratte, F., 1976. The near-real-time, global, four-dimensional analysis experiment during the GATE period, Part I. Journal of the Atmospheric Sciences 33, 561–591.

Monteiro, A., Ribeiro, I., Tchepel, O., Sá, E., Ferreira, J., Carvalho, A., Martins, V., Strunk, A., Galmarini, S., Elbern, H., et al., 2013. Bias correction techniques to improve air quality ensemble predictions: focus on O3 and PM over Portugal. Environmental Modeling & Assessment 18, 533–546.

Morel, P., Talagrand, O., 1974. Dynamic approach to meteorological data assimilation. Tellus 26, 334–344.

Morelli, X., Rieux, C., Cyrys, J., Forsberg, B., Slama, R., 2016. Air pollution, health and social deprivation: A fine-scale risk assessment. Environmental research 147, 59–70.

Munoz-Alpizar, R., Pavlovic, R., Moran, M.D., Chen, J., Gravel, S., Henderson, S.B., Ménard, S., Racine, J., Duhamel, A., Gilbert, S., et al., 2017. Multi-year (2013–2016) PM2.5 wildfire pollution exposure over North America as determined from operational air quality forecasts. Atmosphere 8, 179.

Nadler, P., Arcucci, R., Guo, Y.K., 2019. Data Assimilation for Parameter Estimation in Economic Modelling, in: 2019 15th International Conference on Signal-Image Technology & Internet-Based Systems (SITIS), IEEE. pp. 649–656.

Navon, I.M., 2009. Data assimilation for numerical weather prediction: a review, in: Data assimilation for atmospheric, oceanic and hydrologic applications. Springer, pp. 21–65.

Nguyen, C.V., 2017. Assimilation de données et couplage d'échelles pour la simulation de la dispersion atmosphérique en milieu urbain. Ph.D. thesis. Lyon.

Nguyen, C.V., Soulhac, L., Salizzoni, P., 2018. Source Apportionment and Data Assimilation in Urban Air Quality Modelling for NO2: The Lyon Case Study. Atmosphere 9, 8.

O'Driscoll, R., ApSimon, H.M., Oxley, T., Molden, N., Stettler, M.E., Thiyagarajah, A., 2016. A portable emissions measurement system (pems) study of nox and primary no2 emissions from euro 6 diesel passenger cars and comparison with copert emission factors. Atmospheric environment 145, 81–91.

Pognant, F., Bo, M., Nguyen, C.V., Salizzoni, P., Clerico, M., 2018. Design, modelling and assessment of emission scenarios resulting from a network of wood biomass boilers. Environmental Modeling & Assessment 23, 157–164.

Rouil, L., Honore, C., Vautard, R., Beekmann, M., Bessagnet, B., Malherbe, L., Meleux, F., Dufour, A., Elichegaray, C., Flaud, J.M., et al., 2009. PREV'AIR: an operational forecasting and mapping system for air quality in Europe. Bulletin of the American Meteorological Society 90, 73–84.

Saikawa, E., Kurokawa, J.i., Takigawa, M., Borken-Kleefeld, J., Mauzerall, D.L., Horowitz, L.W., Ohara, T., 2011. The impact of China's vehicle emissions on regional air quality in 2000 and 2020: a scenario analysis. Atmospheric Chemistry and Physics .

Salem, N.B., Garbero, V., Salizzoni, P., Lamaison, G., Soulhac, L., 2015. Modelling pollutant dispersion in a street network. Boundary-Layer Meteorology 155, 157–187.

Salizzoni, P., Grosjean, N., Méjean, P., Perkins, R., Soulhac, L., Vanliefferinge, R., 2007. Wind tunnel study of the exchange between a street canyon and the external flow, in: Air Pollution Modeling and Its Application XVII. Springer, pp. 430–437.

Salizzoni, P., Soulhac, L., Mejean, P., 2009. Street canyon ventilation and atmospheric turbulence. Atmospheric Environment 43, 5056–5067.

Segers, A., Heemink, A.W., Verlaan, M., van Loon, M., 2000. A modified RRSQRT-filter for assimilating data in atmospheric chemistry models. Environmental Modelling & Software 15, 663–671.

Seinfeld, J.H., 1986. Atmospheric chemistry and physics of air pollution. Willey Interscience, New York 738.

Silver, J.D., Brandt, J., Hvidberg, M., Frydendall, J., Christensen, J.H., 2013. Assimilation of OMI NO2 retrievals into the limited-area chemistry-transport model DEHM (v2009. 0) with a 3-D OI algorithm. Geoscientific Model Development 6, 1–16.

Smit, R., Poelman, M., Schrijver, J., 2008. Improved road traffic emission inventories by adding mean speed distributions. Atmospheric Environment 42, 916–926.

Soulhac, L., 2000. Modélisation de la dispersion atmosphérique à l'intérieur de la canopée urbaine. Ph.D. thesis. Lyon.

Soulhac, L., Garbero, V., Salizzoni, P., Mejean, P., Perkins, R., 2009. Flow and dispersion in street intersections. Atmospheric Environment 43, 2981–2996.

Soulhac, L., Nguyen, C.V., Volta, P., Salizzoni, P., 2017. The model sirane for atmospheric urban pollutant dispersion; PART III: Validation against NO2 yearly concentration measurements in a large urban agglomeration. Atmospheric Environment 167, 377–388.

Soulhac, L., Perkins, R.J., Salizzoni, P., 2008. Flow in a street canyon for any external wind direction. Boundary-Layer Meteorology 126, 365–388.

Soulhac, L., Salizzoni, P., Cierco, F.X., Perkins, R., 2011. The model SIRANE for atmospheric urban pollutant dispersion; part I, presentation of the model. Atmospheric environment 45, 7379–7395.

Soulhac, L., Salizzoni, P., Mejean, P., Didier, D., Rios, I., 2012. The model SIRANE for atmospheric urban pollutant dispersion; PART II, validation of the model on a real case study. Atmospheric environment 49, 320–337.

Soulhac, L., Salizzoni, P., Mejean, P., Perkins, R.J., 2013. Parametric laws to model urban pollutant dispersion with a street network approach. Atmospheric Environment 67, 229–241.

Tilloy, A., Mallet, V., Poulet, D., Pesin, C., Brocheton, F., 2013. Blue-based NO2 data assimilation at urban scale. Journal of Geophysical Research: Atmospheres 118, 2031–2040.

Tombette, M., Mallet, V., Sportisse, B., 2009. PM10 data assimilation over europe with the optimal interpolation method .

UNION, P., et al., 2008. Directive 2008/50/EC of the European Parliament and of the Council of 21 May 2008 on ambient air quality and cleaner air for Europe. Official Journal of the European Union .

Wang, X., Mallet, V., Berroir, J.P., Herlin, I., 2011. Assimilation of OMI NO2 retrievals into a regional chemistry-transport model for improving air quality forecasts over Europe. Atmospheric environment 45, 485–492.

Wilczak, J., McKeen, S., Djalalova, I., Grell, G., Peckham, S., Gong, W., Bouchet, V., Moffet, R., McHenry, J., McQueen, J., et al., 2006. Bias-corrected ensemble and probabilistic forecasts of surface ozone over eastern North America during the summer of 2004. Journal of Geophysical Research: Atmospheres 111.

Wu, L., Mallet, V., Bocquet, M., Sportisse, B., 2008. A comparison study of data assimilation algorithms for ozone forecasts. Journal of Geophysical Research: Atmospheres 113.

Zhou, G., Xu, J., Xie, Y., Chang, L., Gao, W., Gu, Y., Zhou, J., 2017. Numerical air quality forecasting over eastern China: An operational application of WRF-Chem. Atmospheric Environment 153, 94–108.